**Pharmacophore**

ISSN-2229-5402

Journal home page: http://www.pharmacophorejournal.com

# NEUROPROTECTIVE ROLE OF MICROBIAL BIOTRANSFORMED METABOLITES OF SINAPIC ACID ON REPETITIVE TRAUMATIC BRAIN INJURY IN RATS

**Samir M. Osman[1], Hesham S. M. Soliman[2,3], Fadila M. Hamed[1], Diaa A. Marrez[4], Amira A. El-Gazar[5], Ahmed S. Alazzouni[6*], Tamer Nasr[7,8], Haitham A. Ibrahim[2]**

1. ***Department of Pharmacognosy, Faculty of Pharmacy, October 6th University.6th of October, 12566. Cairo, Egypt.***
2. ***Department of Pharmacognosy, Faculty of Pharmacy, Helwan University, Ein Helwan, 11795, Cairo, Egypt.***
3. ***Pharm D program, Egypt-Japan University of science and technology, New Borg El-Arab City, 21934, Egypt.***
4. ***Department of Food Toxicology and Contaminants, National Research Centre, Cairo, Egypt.***
5. ***Department of Pharmacology & Toxicology, Faculty of Pharmacy, October 6th University.6th of October, 12566. Cairo, Egypt.***
6. ***Department of Zoology, Faculty of Science, Helwan University, Ein Helwan, 11795, Cairo, Egypt.***
7. ***Department of Pharmaceutical Chemistry, Faculty of Pharmacy, Helwan University, 11795 Helwan, Cairo, Egypt.***
8. ***Department of Pharmaceutical Chemistry, Faculty of Pharmacy, Modern University for Technology and Information, Egypt.***

**ARTICLE INFO**

**Received:**
18 Jul 2022
**Received** in revised form:
19 Oct 2022
**Accepted:**
24 Oct 2022
**Available online:**
28 Oct 2022

***Keywords:*** Gallic, Protocatechuic, Ferulic acids, Sinapic acid, Neuroprotective, Repetitive traumatic

**ABSTRACT**

Sinapic acid biotransformation was studied and screened using eleven fungal cultures. *Penicillium chermesinum* AUMC 275, *Aspergillus ochraceus* AUMC 11328, and *Paecilomyces variotii* AUMC 5618 showed positive results in the production of metabolites. Sinapic acid biotransformation resulted in the production of gallic acid after 10 days incubation with *P. chermesinum*, protocatechuic acid after 7 days with *A. ochraceus*, and ferulic acid after 5 days with *P. variotii*. The investigated compounds' anti-inflammatory efficacy results, as well as the suggested binding mechanism, affinity, preferred orientation of each docking pose, and binding free energy with the GSK-3β enzyme, were predicted using molecular modeling. The predicted interaction energies for the examined chemicals agreed with the experimental findings. Moreover, we evaluated the neuroprotective potential of the obtained metabolites using the mild repetitive traumatic brain injury (mRTBI) model. Animals were exposed to 5 repetitive hits once per day by weight drop device and were divided into 6 groups (control, mTBI, mRTBI-10, mRTBI-10+Fa, mRTBI-10+PCA, mRTBI-10+GA). All the treatments decreased cortical contents of Tau protein (dementia marker), inflammatory markers (TNF-α and il-6), and signaling molecules such as GSK3B and DKK-1. Furthermore, the histological findings added another neuroprotective potential of obtained metabolites where marked improvements and ameliorative effect on the histoarchtexture of the hippocampus and mild changes in the hippocampus layers by GA, PCA, and FA, respectively. All these effects were mirrored in behavior outcomes, and a significant enhancement in animal behavior was observed. We concluded that GA, PCA, and FA have therapeutic potential for preventing TBI-induced brain injury.



**To Cite This Article:** Osman SM, Soliman HSM, Hamed FM, Marrez DA, El-Gazar AA, Alazzouni AS, et al. Neuroprotective Role of Microbial Biotransformed Metabolites of Sinapic Acid on Repetitive Traumatic Brain Injury in Rats. Pharmacophore. 2022;13(5):112-26. https://doi.org/10.51847/1Rj6v3EGdU

**Corresponding Author:** Ahmed S. Alazzouni; Department of Zoology, Faculty of Science, Helwan University, Ein Helwan, 11795, Cairo, Egypt. E-mail: drahmedalazzouni@gmail.com.

## Introduction

The global health issue of traumatic brain injury (TBI) affects millions of people each year [1, 2]. Chronic brain conditions such as chronic traumatic encephalopathy (CTE) are more likely to develop in later life due to repeated TBI exposure [3]. CTE can arise from contact sports and military contribution [4]. Hence**,** growing awareness has focused on the neurological sequelae of sports-related head trauma, particularly concussions. Most of them are associated with behavioral deficits such as mood, cognition, and gait disturbances, which are recently categorized as neurodegenerative disorders [5, 6]. However, the whole picture that environs this neurodegenerative disease/syndrome is still unknown. Although some steps/phases have unveiled part of the formidable pathological process after RTBI/CTE, the presence of an effective pharmacological therapy remains challenging. Therefore, one of the current study's aims is to evaluate the potential neuroprotective effect of the natural biotransformed metabolites on the behavioral and biochemical changes developed in the repetitive traumatic brain injury (RTBI) model.

Biotransformation is the process by which organisms or enzyme systems change the structural properties of a chemical substance, resulting in the conversion of one component into another. This method, which bacteria have developed to adapt to environmental changes, is helpful in various biotechnological operations. These reactions are crucial for putting chemical functions into molecules' inaccessible locations and creating unusual structures. Because of its straightforward, affordable, and safe approaches that combine green chemistry with high efficiency, biotransformation has attracted a lot of attention [7].

A minor naturally occurring hydroxycinnamic acid derivative is called sinapic acid. It belongs to the phenylpropanoid family of phenolic compounds, which is thought to have medicinal benefits and is generally harmless. Sinapic acid is a common component of the human diet. It is found in various plants, including fruits, vegetables, cereal grains, oilseed crops, spices, and medicinal herbs. Sinapic acid exhibits a broad range of biological actions, including hepatoprotective, anti-cancer, antioxidant, anti-inflammatory, antibacterial, and anti-inflammatory effects [8].

In this work, we explored the capability of 11 fungal cultures to biotransform sinapic acid into new products. Also, we evaluated the neuroprotective/anti-inflammatory activity of the obtained metabolites, namely gallic acid, protocatechuic acid, and ferulic acid, using the repetitive traumatic brain injury (RTBI) model. This was done by applying 5 repetitive blows on the right anterior frontal area of the right cortex and then left for 10 days to compare the effect of treatments that lasted for 10 days.

## Materials and Methods

*Instruments and Materials for Microbial Biotransformation*

Sabouraud-dextrose agar (SDA) Becton Dickinson and Company, Cockeysville, Maryland 21030 Yeast extract of a high microbial standard (Oxoid LTD, England); microbiological grade peptone (Sigma Chemical Co., USA); agar with potato dextrose (DIFCO, USA); Dextrose, grade AR (Sigma Chemical Co., USA); glycerol, dipotassium hydrogen phosphate, and analytical-grade sodium chloride (ADWIC, Egypt); Mineral agar (Oxoid LTD, England); Sinapic acid originated in St. Louis, USA (Sigma Aldrich); (ScoutTM Pro (OHAUS) model, USA); Digital balance AutoclavePb1 (Germany); bath of sonicated water (Branson 3510E-MTH, Mexico); Incubator with gyratory motion (Lab Line Instrument, USA); Oven with a thermostat, WT-binder 7200 (Germany). *Aspergillus alliaceous* NRRL315, *Aspergillus niger* NRRl3, *Penicillium chrysogenum* ATCC 948, *Aspergillus flavus* AUMC 4787, *Aspergillus awamori* AUMC58, *Aspergillus ochraceous* AUMC11328, *Penicillium chermesinum*AUMC275, *Cunningamella blackeseleeana* AUMC5618, *Paecilomyces variotii* AUMC4807 and *Aspergillus versicolor* NRRL 1306 were obtained from American Type culture collection (ATCC), Northern Regional Research Laboratories (NRRL) and Assiut University Mycological center (AUMC).

*Small Scale Biotransformation of Sinapic Acid*

The small-scale screening studies were conducted following a two-stage fermentation technique [9]. The metabolites were found using TLC with the solvent system methylene chloride, methanol (9:1 V/V), and by spraying anisaldehyde/sulfuric acid reagent and vanillin/sulfuric acid.

*Large-Scale Biotransformation of Sinapic Acid*

After conducting initial exploratory screening tests employing Penicillium chermesinm AUMC275, Aspergillus ochraceus AUMC11328, and Paecilomyces variotii AUMC4807 cultures, which produced positive screening results, large-scale transformation of sinapic acid was carried out. For each experiment, sinapic acid (1 g) was dissolved in 10 ml of DMSO and distributed evenly among 10 flasks (each holding 1000 ml) containing 200 ml of stage II culture. The cultures were then allowed to develop at 25 ± 2 °C on a gyratory shaker at 100 rpm after the appropriate time for each experiment (5, 7, and 10 days). The recovered, filtered liquid media underwent thorough ethyl acetate extraction. The extracts were combined and evaporated to dryness to give 3.4 g (**FI**) residue for*penicilliumchermesinm*AUMC275 experiment, 3 g (**FII**) for *Aspergillus ochraceous* AUMC11328 experiment, and 3.6g for (**FIII**).

The NMR spectra were captured with a Bruker 400 MHz for 1H NMR and a 100.40 MHz for $^{13}C$ NMR. As an internal reference, chemical shifts were reported as δ ppm relative to tetramethylsilane (TMS). The spectra were conducted in DMSO. Rotational evaporator (BUECHI, Germany). Laminar-flow canopy (EACT 8613, USA). Fluorescence analysis

cabinet with a UV lamp and spectroline (R) Model M-10 (USA). Column chromatography was used with silica gel G 60, 70, or 230 mesh (Merck, Germany). Aluminum sheets with silica gel G $F_{254}$ precoat underwent TLC (Merck, KGaA, Darmstadt, Germany). Anisaldehyde/sulfuric acid reagent was sprayed on developed chromatograms to make them visible. Solvent solutions were used in the development of TLC plates. Methanol and methylene chloride (DCM) are present in the ratios of (**$S_1$**) (9:1 V/V), (**$S_2$**) (9.5:0.5 V/V), and (**$S_3$**) (8:2 V/V).

*Isolation and Purification of the Metabolites*

Each 1g of substrate for every experiment gives **FI** (3.4 g), **FII** (3g), and **FIII** (3.6 g) was chromatographed separately on a silica gel column (100g 3cm×60cm) using the dry method. Starting with hexane and moving through hexane/DCM mixes with increasing polarity up to 100% DCM and then DCM/MeOH mixtures with increasing polarity up to 50% MeOH, the columns were eluted in a gradient fashion. After purification on a Sephadex column, **FI** gave a 21% yield, **FII** offered a 19.5% yield, and **FIII** gave a 20% yield.

*In Vivo Anti-Inflammatory Study*

*Materials for the Anti-Inflammatory Activity*

4% Isoflurane, We obtained adult male Sprague-Dawley rats from the National Research Center (NRC, Giza, Egypt) and DMSO (FINE-CHEM Limited, India).

*Tissue Preparation and ELISA Assessment*

Animals in the first set (n=6/group) were sacrificed, and the right cerebral cortex was collected and homogenized in phosphate buffer for ELISA measurement. ELISA kits were used for the measurement of the homogenate contents of the dementia marker [phosphorylated tau (p-Tau; MyBioSource, CA, USA)], signaling molecules [glycogen synthase-3beta (GSK-3β; Invitrogen Corporation: Camarillo, CA), Dickkopf -1(DKK-1; MyBioSource, CA, USA), and inflammatory biomarkers [tumor necrosis-alpha factor (TNF-α; Ray Biotech, GA, USA), interleukin-6 (IL-6; R&D Systems, CH)] according to the manufacturer's instructions provided.

*Animal Care and Maintenance*

Throughout the study, 114 mature male Sprague-Dawley rats (n = 114), weighing 250–300 g, were housed in cages with 5 rats each under standard laboratory conditions (controlled temperature, humidity, ventilation, and a 12-hour light/dark cycle) with unrestricted food and water. Rats were given at least a week to acclimate to the vivarium before any experimental operations. When handling the animals, the Guide for the Care and Use of Laboratory Animals was rigorously followed (NIH publication, 1996).

*Induction of Mild Single and Repetitive Trauma*

The weight drop device was used to induce the trauma [10], but with a few modifications learned from our earlier research [11]. All of the animals in the six groups had 4% isoflurane anesthesia before being put on the platform directly beneath the weight drop apparatus. Throughout the experiment, isoflurane vaporized at a concentration of 1.5% and was inhaled through a mask to maintain anesthesia. Except for the normal control group, the impact region was chosen to be the right anterior frontal area, 1.5 mm lateral to the midline in the mid-coronal plane. A weight of 75 g was released and dropped with a final impact of 0.5 J onto the skull.

*Experimental Design*

The animals were separated into six groups (n = 19), with six rats used for biochemical assays, ten rats used for behavioral experiments, and the remaining three rats maintained for histopathological analysis. These sets were chosen based on findings from our earlier study11, in which the brains of animals subjected to behavioral tests lost consistency compared to their mates who were not subjected to these tests. The rats in this group were subjected to 5 days of isofluorane exposure as a negative control. Animals in group 2 were given one blow and slaughtered after 24 hours to act as the mTBI control group. Animals in group 3 were exposed to 1 blow for 5 days and then left for 10 days to compare the effect of treatments that lasted for 10 days after the last fifth blow, and they were signified as mRTBI-10. In group 4, animals in this group were subjected to the 5 hits as those in group 3 and then received 100 mg/kg ferulic acid immediately after the last hit [12], and then left for ten days without further administration of the drug. Group 5, immediately after the 5th hit, protocatechuic acid (30 mg/kg) was given i.p and then continued once per day to reach one week of treatment [13]. In Group 6, gallic acid was injected (10 mg/kg; i.p) 1 h after the 5th the last hit, which continued for 10 days [14].

*Open Field Test*

At the end of the experiment, animals in the second set were subjected to the open field test, which depends on measuring locomotor activity, emotionality, and exploratory behavior utilizing latency time, ambulation frequency, rearing frequency, and grooming frequency for 3min. Animals were put independently in the central point of the open field mechanical device and permitted to move unreservedly around the open field to investigate nature for three minutes for examination purposes.

A camcorder precisely recorded all The actions during these 3 mins, and the accompanying previously mentioned parameters were watched [15].

*Molecular Modeling*

The crystal structure of Glycogen Synthase Kinase-3 in combination with AR-A014418 as an inhibitor (PDB ID: 1Q5K) was chosen as the template for molecular modeling investigation by Molecular Operating Environment (MOE®). 2014.09 version (Chemical Computing Group Inc., Montreal, Canada). The enzyme was prepared for docking studies by removing chain B of its dimer, water molecules, and ligands that are not involved in binding and adding missing hydrogen atoms. The active docking site was defined using the co-crystallized ligand. The docking methodology employed the Triangle Matcher Placement method and the London dG score function. The protein was minimized with MOE until an RMSD gradient of 0.05 kcal·mol$^{-1}$Å$^{-1}$ was achieved using the MMFF94x force field, and the partial charges were determined automatically.

*Statistical Analysis*

All data are presented as mean ± S.D. The means of the (n = 6 or 10) were statistically compared using one-way ANOVA, followed by Tukey's post hoc test. GraphPad Prism software (version 5.0 d; GraphPad Software, Inc., San Diego, CA, USA) was used for all statistical tests, and P <0.05 was used as the significance level.

**Results and Discussion**

*Structure Elucidation of Isolated Metabolites*

Metabolite **1** was obtained as an off-white amorphous powder (170 mg). The $R_f$ - value was 0.52 ($S_3$), and it appeared as a dark purple spot under short UV light and showed violet fluorescence under long UV light. It gave blue color with $FeCl_3$ Spray reagent.$^1$H NMR (400 MHz, DMSO-$d_6$), δ ppm 6.88 (2 H, s, H-2/6). $^{13}$C NMR (100 MHz, DMSO-$d_6$), δ ppm 168.59 (C=O), 146.09 (C-3/5), 138.48 (C-4), 121.80 (C-1), 121.80 (C-2/6). Negative ESI-MS showed a molecular ion peak at 169.11 [M-H], which corresponded to a Mwt of 170. $^1$H NMR and $^{13}$C NMR, and ESI-MS data agreed with the reported data [16]. Accordingly, the compound was confirmed to be gallic acid, see **Figure 1a**.

Metabolite **2** was obtained as an off-white amorphous powder (167mg). $R_f$- value 0.66 ($S_1$); it gave dark spots under short UV-light and shiny violet fluorescent spots under long UV light. $^1$H NMR (400 MHz, $CD_3OD$), δ ppm 7.45 (1 H, d, *J*= 1.69, H-2), 7.43 (1 H, dd, *J*= 1.69, 8.34, H-6), 6.79 (1 H, d, *J*= 8.23, H-5). $^{13}$C NMR (100 MHz, DMSO-$d_6$), δ ppm 167.61 (C-7), 149.85 (C-4), 144.79 (C-3), 122.05 (C-6), 121.85 (C-1), 116.58 (C-2), 115.12 (C-5). Negative ESI-MS showed a molecular ion peak at 153.14[M-H]$^-$. All proton and carbon recorded resonances are in good agreement with that of protocatechuic acid **(Figure 1a)** by comparing data with that isolated before [17].

Metabolite **3** was isolated as an off-white amorphous powder (175 mg). $R_f$- value 0.64 ($S_2$); it showed a dark purple spot under short UV-light and shiny violet fluorescence under long UV light. $^1$H NMR (400 MHz, DMSO-$d_6$), δ ppm 7.08 (H, dd, *J*= 8.19, 1.93, H-6), 7.28 (1 H, d, *J*= 1.90, H-2), 6.79 (1 H, d, *J*= 8.06, H-5), 7.49 (1 H, d, *J*= 15.89, H-7), 6.36 (1 H, d, *J*= 15.88, H-8), 3.81 (3 H, s, O-$CH_3$). $^{13}$C NMR (100 MHz, DMSO+-$d_6$), of δ ppm 168.55 (C-9), 149.64 (C-4), 148.47 (C-3), 145.07 (C-7), 126.33 (C-1), 123.40 (C-6), 116.18 (C-2), 116.06 (C-8), 111.69 (C-5), 56.24 ($OCH_3$). All proton and carbon resonances are in agreement with that of ferulic acid that was isolated and identified before (Rho and Yoon 2017). Negative ESI-MS spectrum confirmed the structure as it showed a molecular ion peak at m/z 193.38 [M-H]$^-$ which is equivalent to a molecular formula ($C_{10}H_{10}O_4$) and a molecular mass 194.06, which was consistent with the M.wt of ferulic acid. Accordingly, the compound was identified as ferulic acid **(Figure 1a)**.

*Molecular Docking Study*

A molecular docking simulation study of gallic, protocatechuic, and ferulic acids, obtained from microbial biotransformation of sinapic acid, was performed to predict the anti-inflammatory activity results. Furthermore, it will aid in understanding the binding mechanisms and diverse interactions between the ligands and the active site of GSK-3β. The most promising compounds are chosen based on the right binding mode and the binding free energy (ΔG). **Table 1** show the outcomes of the molecular docking, **(Figures 1b-1e)**. Glycogen synthase kinase-3β (GSK-3β) is a serine/threonine kinase that controls various signaling pathways. Among the many tasks that GSK-3β controls, inflammation has recently become one of the most intriguing. TNFα, IL-6, and MCP-1 are examples of pro-inflammatory cytokines and chemokines that are expressed due to an increase in NF-κB activity that GSK-3β mediates. The simultaneous reduction in IL-10 expression makes GSK-3β inhibition protective against inflammatory conditions [18, 19]. Gallic acid inhibits the GSK-3β enzyme and Wnt/β-catenin signaling pathway [20]. In focal cerebral ischemia injury, ferulic acid controls the Akt/GSK-3β/CRMP-2 signaling pathway, preventing brain damage, whereas protocatechuic acids cause GSK-3β inhibition [21].

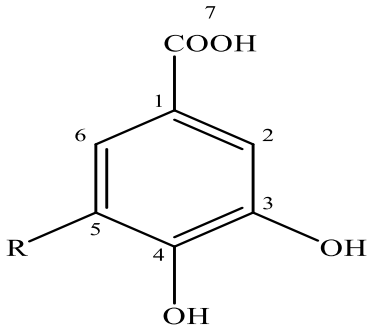


Metabolite **1** R= OH Metabolite **2** R= H

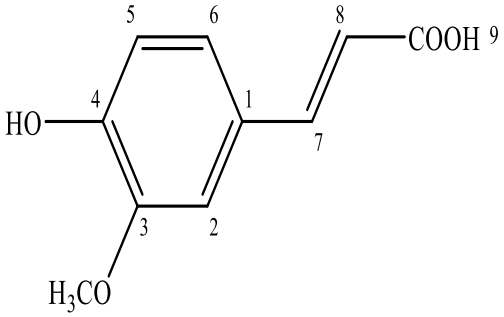


Metabolite **3**

a)

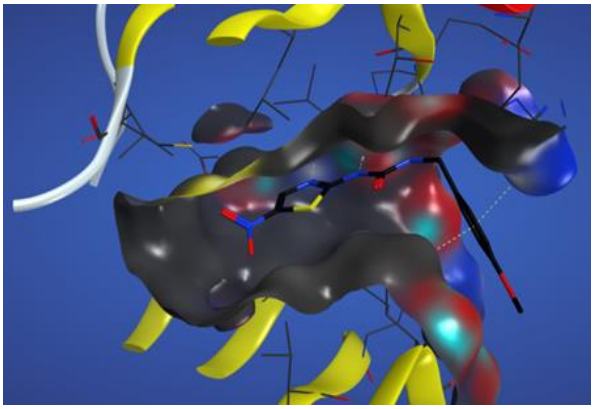

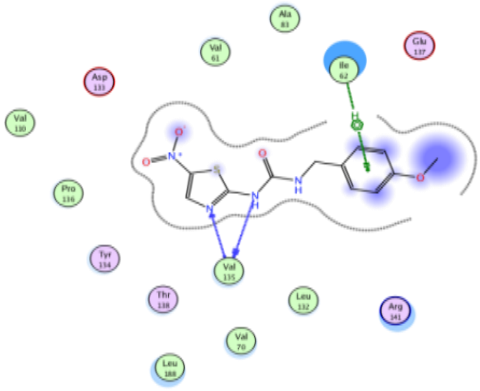


b)

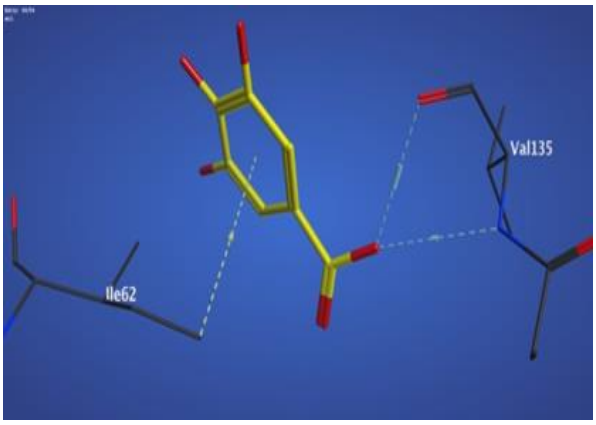


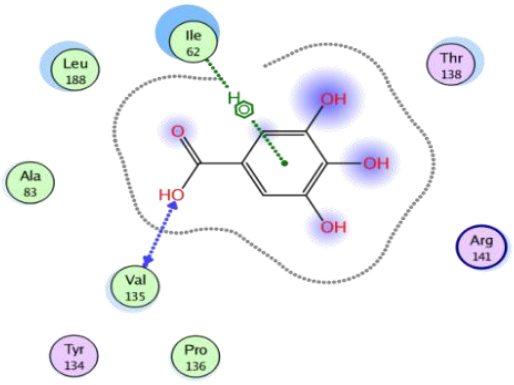


c)

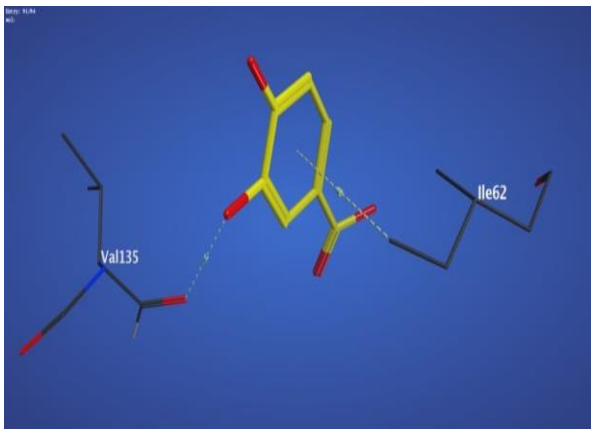


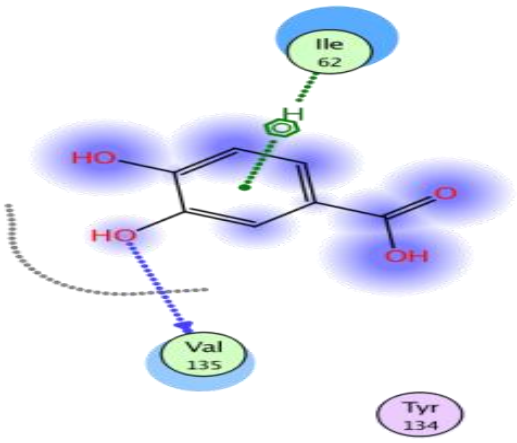


d)

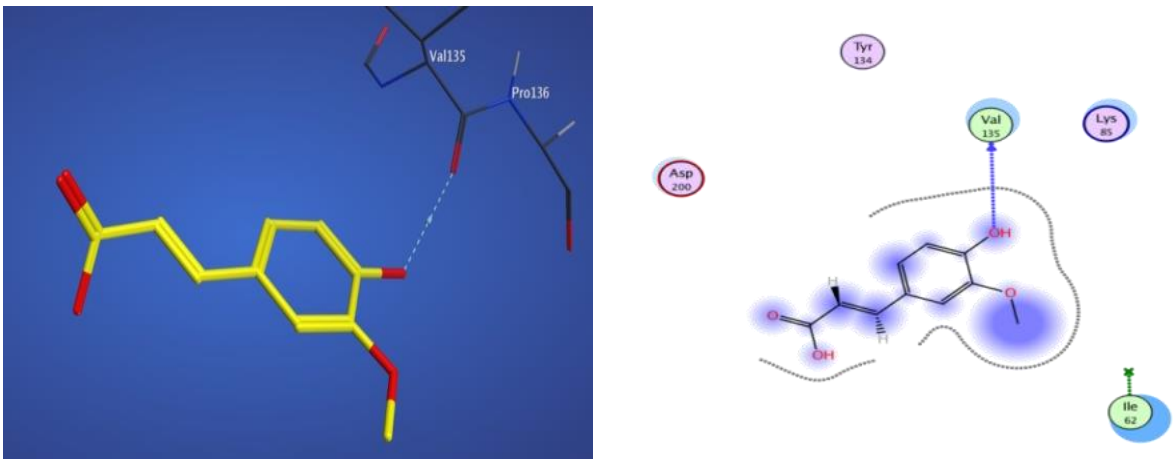


e)

**Figure 1.** a) Chemical structure of the isolated metabolites; b) Surface map of AR-A014418 (black) co-crystallized with GSK-3β (1Q5K) (left); and the corresponding interaction diagram (right); c) Predicted binding mode of gallic acid with the active site of GSK-3β; d) Predicted binding mode of protocatechuic acid with the active site of GSK-3β; e) Predicted binding mode of ferulic acid with the active site of GSK-3β.

**Table 1.** The affinity scores and interactions of the tested compounds and reference drug against GSK-3β (in Kcal/mole)

| Compound | Score | Interaction |
|---|---|---|
| **Gallic acid** | -5.02 | VAL135: Hydrogen –donor<br>VAL135: Hydrogen –acceptor<br>Ile62: Arene-H interaction |
| **Protocatechuic acid** | -4.55 | VAL135: Hydrogen –donor<br>Ile62: Arene-H interaction |
| **Ferulic acid** | -4.31 | VAL135: Hydrogen –donor |
| **AR-A014418** | -5.21 | VAL135: Hydrogen –donor<br>VAL135: Hydrogen –acceptor<br>Ile62: Arene-H interaction |

*Anti-Inflammatory Activity*

*Changes in Cortical Phosphorylated TAU (PTAU)*

The cortical content of pTau was markedly increased in all the animals exposed to 5 hits and left for ten days compared to single traumatized and healthy animals. Compared to the mRTBI-10 insult, all our drug regimens showed anti-dementia properties by decreasing pTau **(Figure 2)**.

**Panel I**

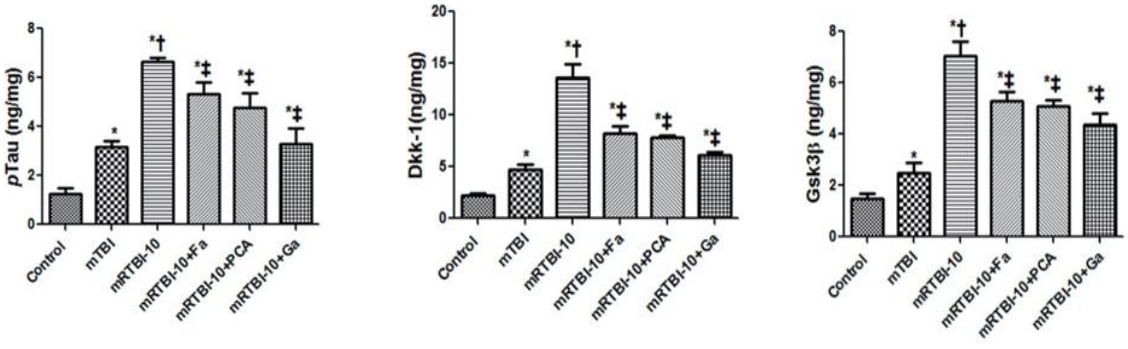


a) b) c)

**Panel II**

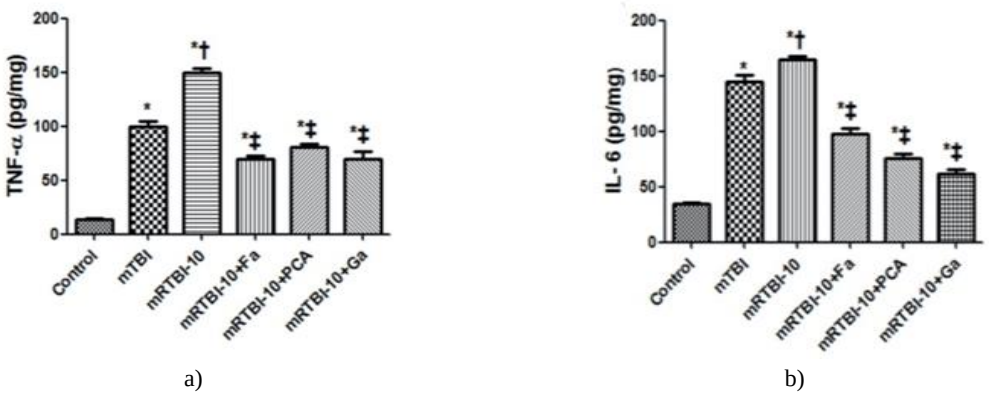


a) b)

**Panel III**

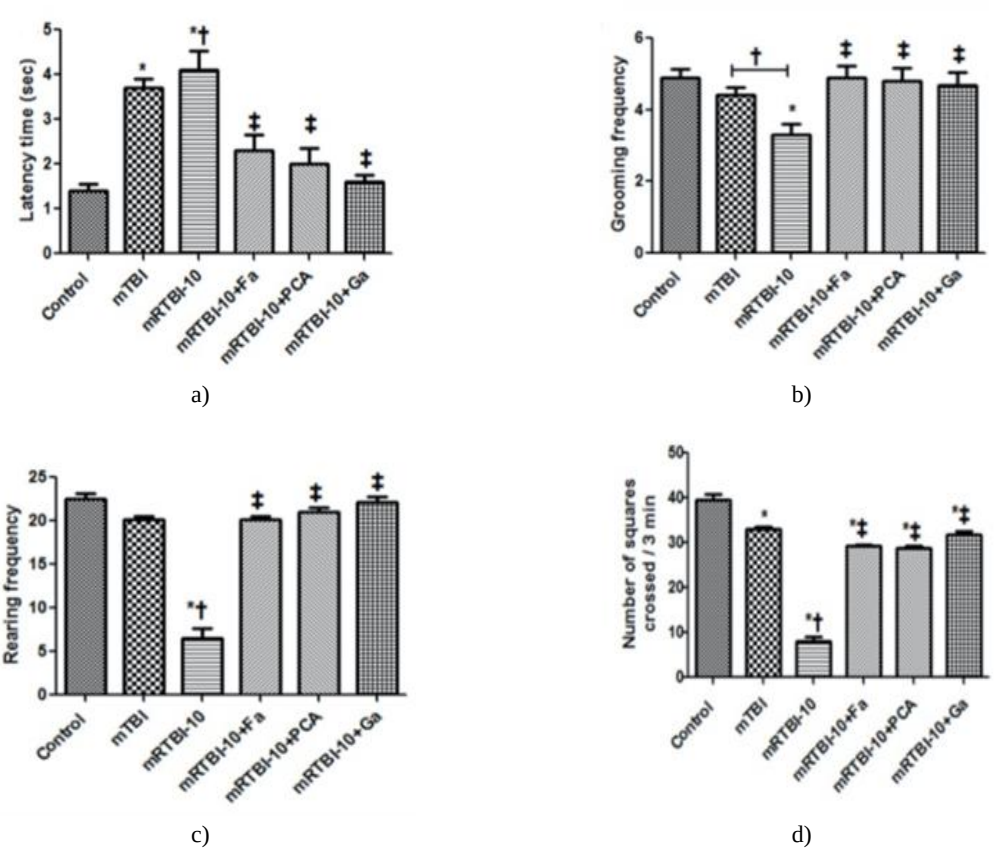


a) b)

c) d)

**Figure 2. Panel I:** the changes of cortical contents of (a) pTau, (b) Dkk-1, and (c) G3K-3. **Panel II:** Changes in the cortical contents of TNF- and IL-6, two inflammatory indicators. **Panel III:** Open field test behavioral changes on (a) latency time, (b) grooming frequency, (c) rearing frequency, and (d) number of squares crossed in 3 minutes. The data are presented as mean (n = 6) SD. The statistical analysis employed one-way ANOVA, and Tukey's post hoc multiple comparison test was run afterward. Relevant to the control group (*), mTBI group (†), and mRTBI-10 group (‡) at P <0.05. Dkk-1 stands for Dickkopf-1, G3K-3 stands for glycogen synthase kinase-3 beta, IL-6 stands for interleukin 6 mTBI, and mRTBI-10 stands for mild traumatic brain injury that occurred 10 days after the fifth blow, and TNF- stands for tumor necrosis factor-alpha.

*Changes in Cortical Dickkopf-1(DKK-1)*

As presented in **Figure 2**, all insults group induced cortical Dkk-1 indicated by 2 folds for mTBI and 6 folds for mRTBI-10, respectively. However, all our drugs abated the elevated Dkk-1 showing neuroprotection against mRTBI-10.

*Changes in Cortical Glycogen Synthase Kinase-3B (GSK-3B)*

Compared to the control group results **(Figure 2)**, the cortical contents of GSK-3β were markedly raised in the single and repetitively traumatized groups. Nevertheless, the post-administration of all the drugs opposed the mRTBI-10 effect, where GSK-3β contents were impeded.

*Changes in Cortical Inflammatory Mediators*

All the traumatized animals (mTBI and mRTBI-10) caused an up-surge of inflammatory mediators, manifested by a notable increase in the cortical content of TNF-α and IL-6 compared to normal animals. These events were significantly revoked by the post-administration of all our drug regimens compared with the mRTBI-10 group **(Figure 2)**.

*Behavioral Changes in Open Field Test*

The results of the open field test indicate that spontaneous locomotor and exploratory activities are disordered due to mRTBI-10. **(Figure 2)** shows that (A) several traumas have lengthened the latency to about 4-5 s and that (B) grooming activities, (C) rearing activities, and (D) the number of squares crossed /3 min were all significantly lower in the mRTBI-10 than in the non-traumatized animals. However, compared to mRTBI-10, all medications significantly increased locomotion and activity after delivery.

*Histopathological Results*

Results of histopathology **(Figures 3-6)**

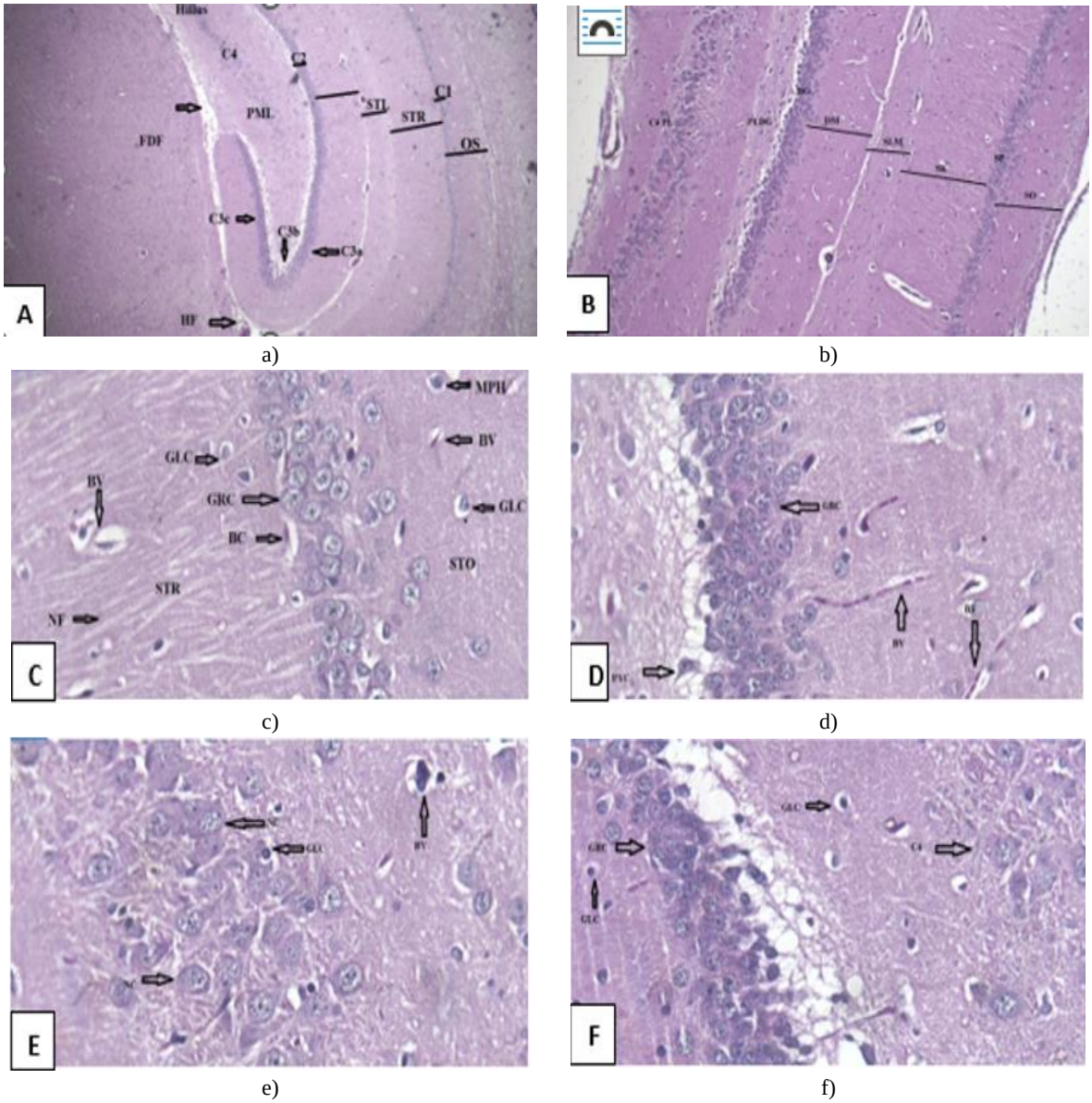


**Figure 3.** photomicrographs of negative control hippocampus showing normal histoarchtexture with normal layers distribution as shown in photo A&B OS; stratum oriens, Sp; stratum pyramidal of CA1, ST, stratum radiatum, SLM; startumlacunosum-molecular, DM; the molecular layer of the dentate gyrus, DG; granule cell layer of the dentate gyrus, PLDG; polymeric layer of the dentate gyrus, C1-3; Field pyramidal layers 1-3; C4; polymorphic layer, FDF; fimbriodentate fissure, HF; hippocampus fissure, other photo C-F showed normal histological structure with GL; glial cells, GC; granular cells, PYC; pyramidal cells, NF; nerve fibers, BC; basket cells and normal vascularization, BV.

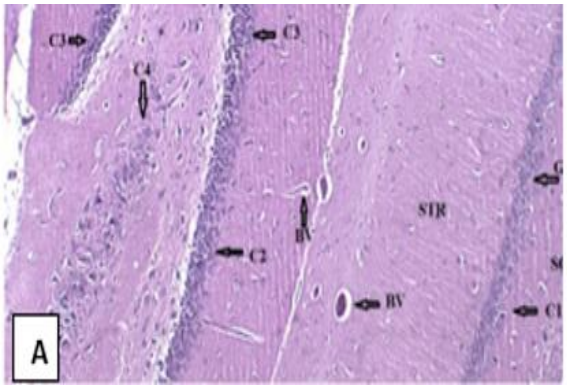
C3
C4
C3
C2
BV
STR
BV
C1
A

a)

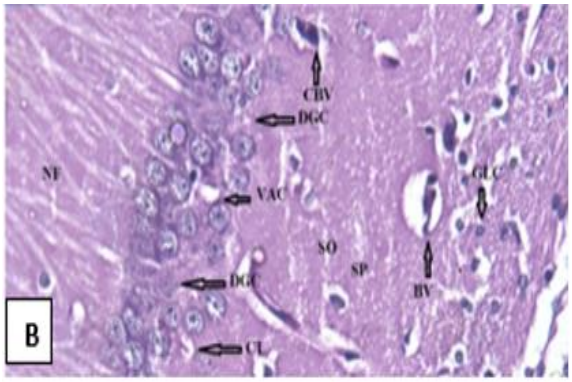
CBV
DGC
NF
VAC
GLC
SO
SP
DGC
BV
CL
B

b)

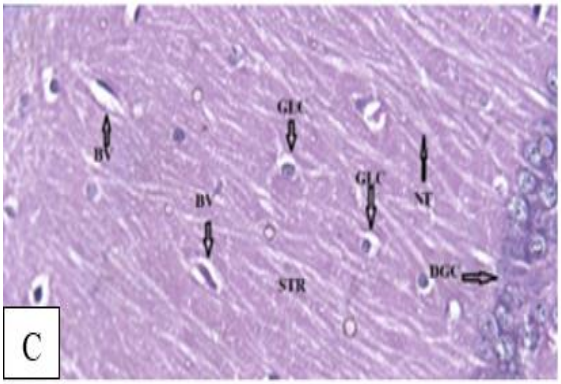
BV
GLC
BV
GLC
NF
STR
DGC
C

c)

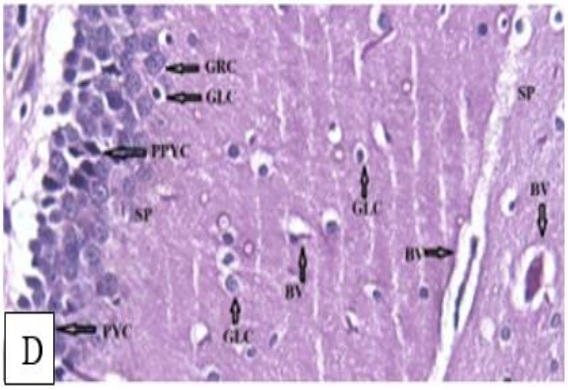
GRC
GLC
SP
PPYC
SP
GLC
BV
BV
BV
PYC
GLC
D

d)

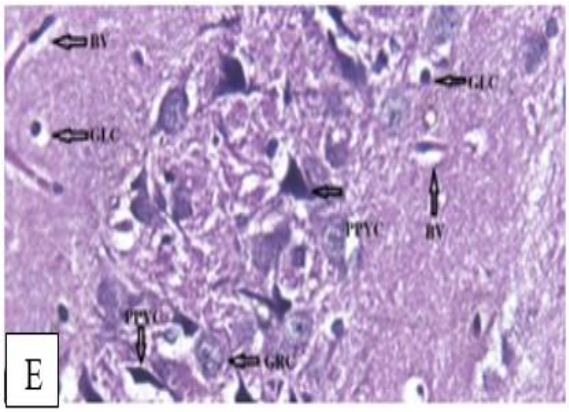
BV
GLC
GLC
PPYC
BV
PPYC
GRC
E

e)

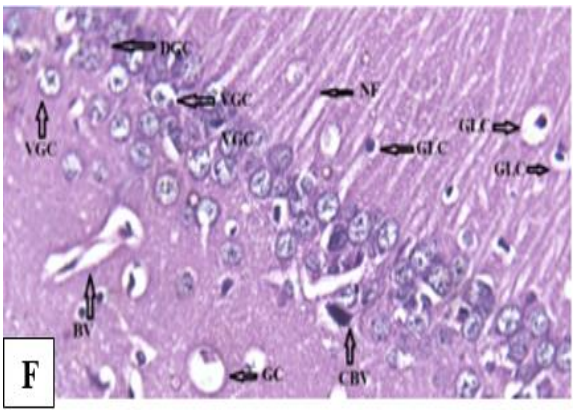
DGC
VGC
NF
VGC
GLC
GLC
GLC
BV
GC
CBV
F

f)

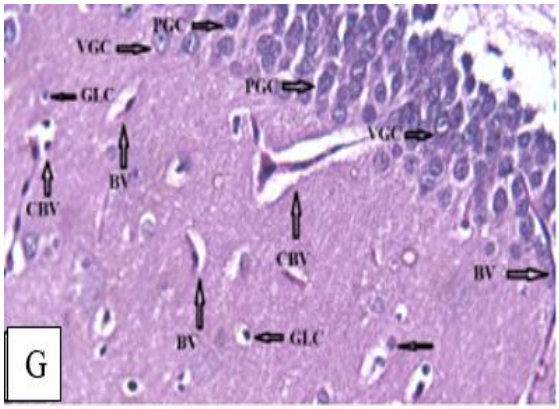
PGC
VGC
GLC
PGC
VGC
CBV
BV
CBV
BV
BV
GLC
G

g)

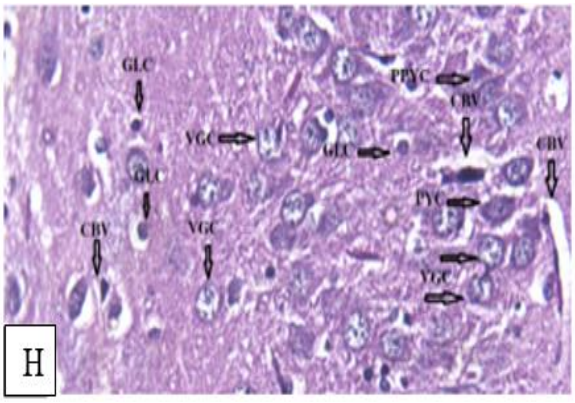
GLC
PPYC
CBV
VGC
GLC
CBV
GLC
PYC
CBV
VGC
VGC
H

h)

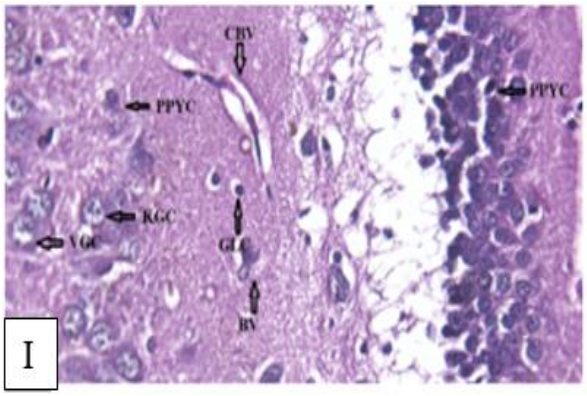


i)

**Figure 4. a-e)** Photomicrograph of MTBI group showed vacuolated granular cells and degenerations VGC, DGC of external granular layer C1 and some pycnotic changes of pyramidal cells PPYC of polymorphic layer C4 and C2 and C3; **f-i)** Photomicrograph of MTBI-10 showed marked vacuolation (VGC) and pyknotic changes of granular cells of both external layer C1 and inner C2 layer and pyknotic changes of pyramidal cells (PPYC) and some karyolysis changes (KGC) of granular cells.

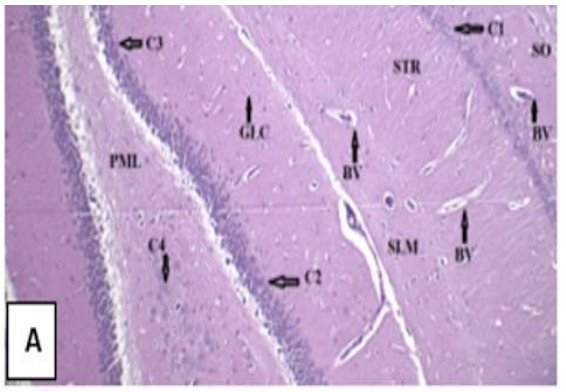


a)

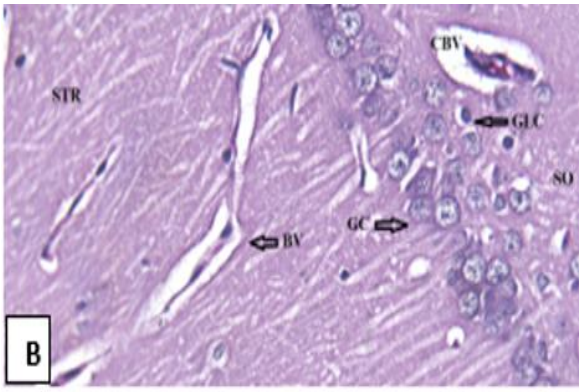


b)

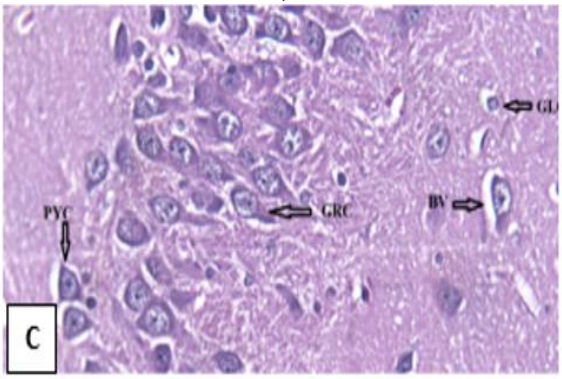


c)

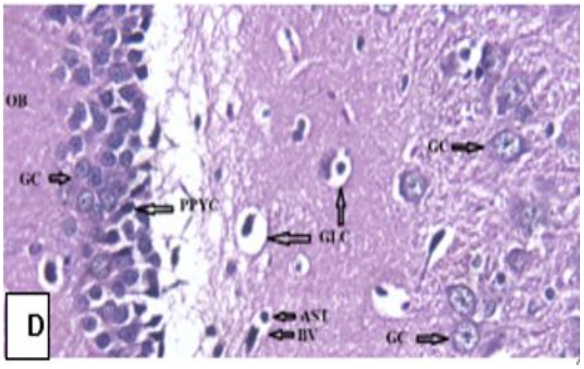


d)

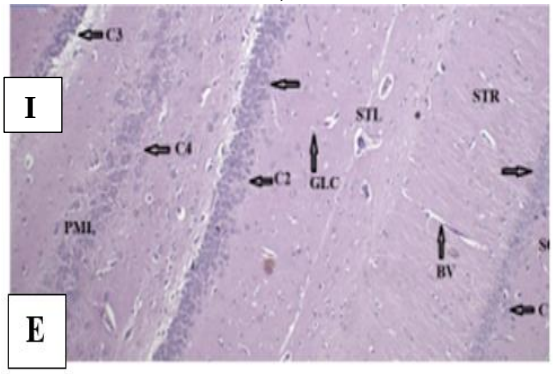


e)

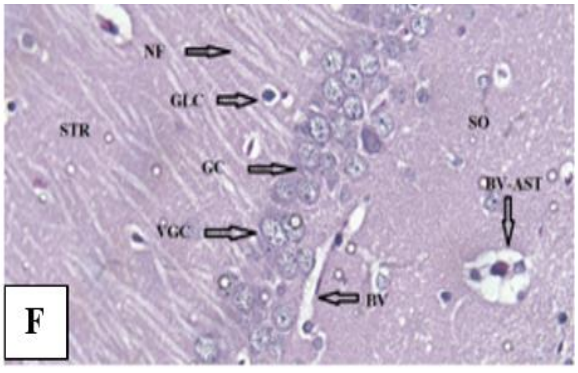


f)

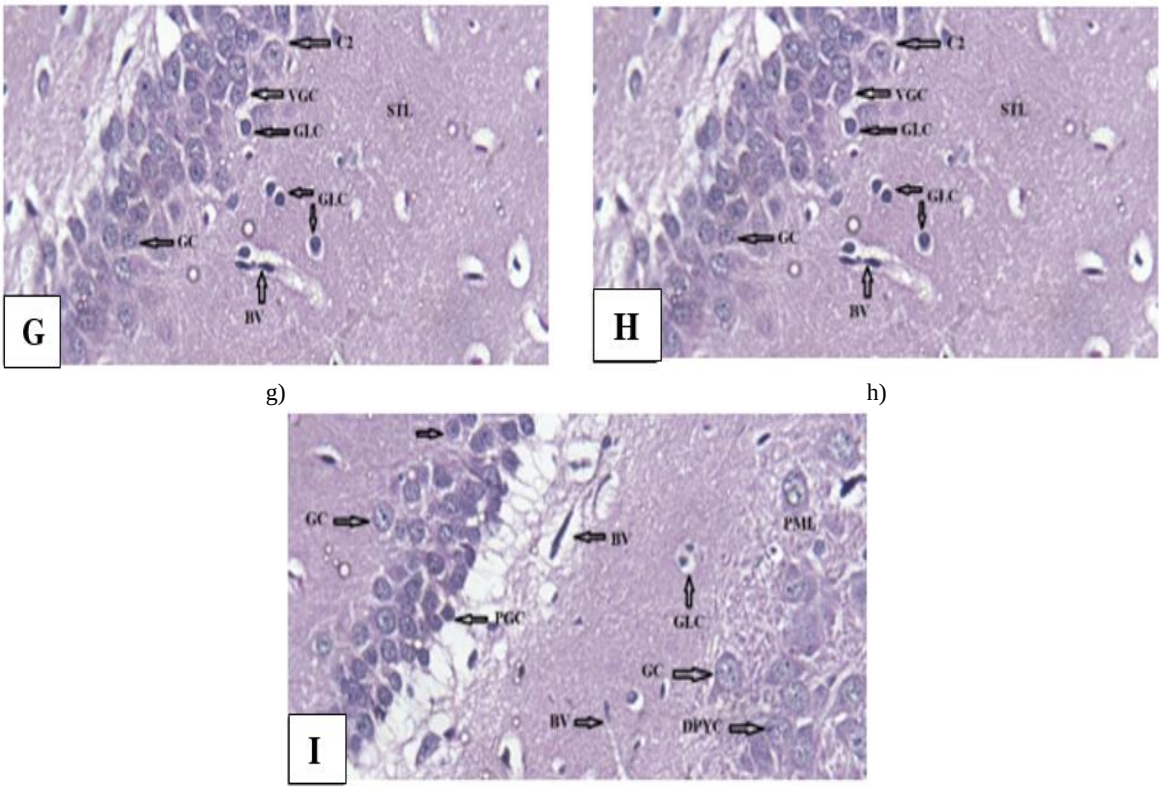


g) h)

i)

**Figure 5. a-d)** Photomicrograph of Gallic acid treated group showed more or less normal histoarchtexture of hippocampus regions with a mild frequency of pyknotic pyramidal cells (PPYC) with normal appearance of neurons and glial cells showing astrocyte (AST) in contact with blood vessel (BV). **e-i)** Photomicrograph of PCA treated group showed mild vacuolations (VGC) pyknotic changes of pyramidal cells and mildly congested blood vessels (BV).

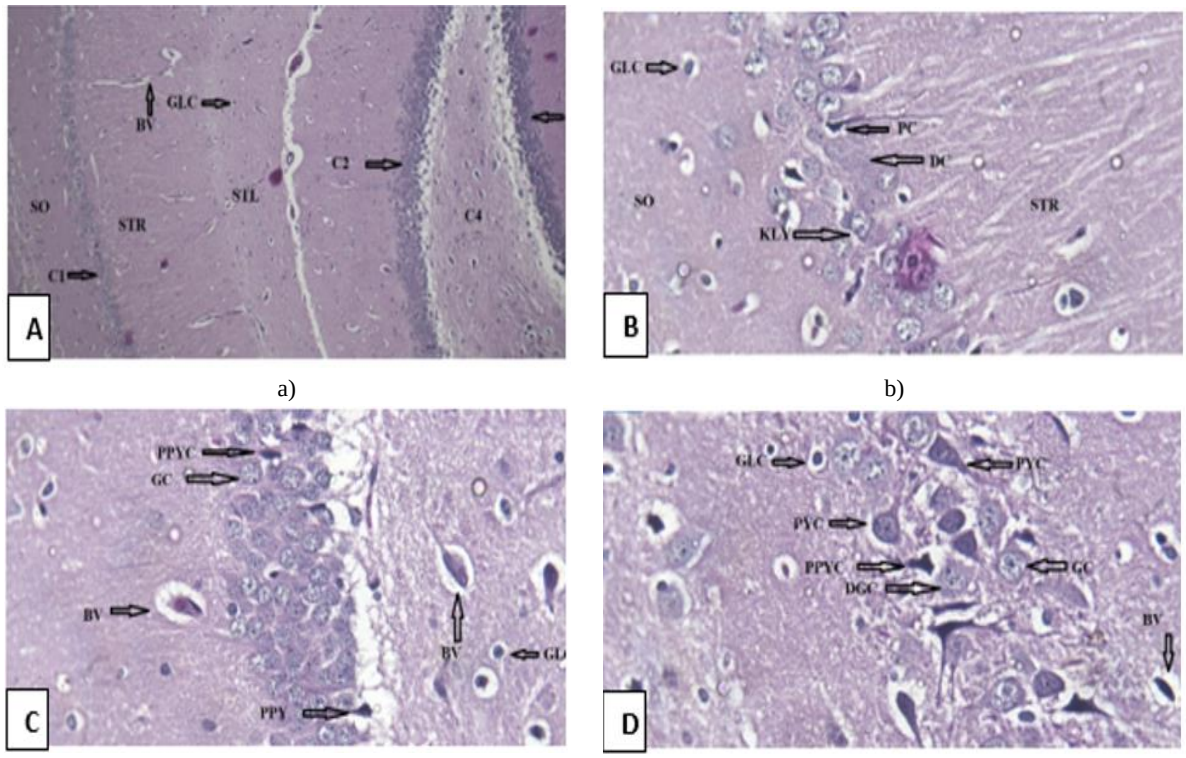


a) b)

c) d)

**Figure 6.** Photomicrograph of the ferulic acid treated group showed mild histological alterations of different regions showed mild pyknotic changes of pyramidal cells (PPYC) with mildly congested blood vessels (BV) and mild granular cell karyolysis (KLY).

*Morphometric Study*

Morphometric study for the measurements of hippocampus layers thickness showed a significant reduction in the thickness of all hippocampus layers in comparison with the negative control group, the most affected layers were stratum Oriens SO., Stratum pyramidal SP. and Stratum lacunosum SLM., while the less affected layers were Stratum Radiatum, molecular dentate gyrus MD, granule dentate gyrus DG, and polymorphic dentate gyrus PL.; both with mTBI or RTBI-10 .as shown in supplementary material attached

After treatment with GA, PCA, and FA, the thickness of all layers increased but was still less than the thickness of normal hippocampus layers. As shown, the most improvement in layer thickness was with GA, PCA, and FA, respectively.

Eleven fungi were tested for their capacity to catalyze the bioconversion of sinapic acid. While Aspergillus ochraceus AUMC11328 culture formed after 7 days of one major metabolite (protocatechuic acid) and Paecilomyces variotii AUMC 5618 culture formed after 5 days of one major metabolite, Penicillium chermesinum AUMC275 culture reproducibly formed after 10 days of incubation of one major metabolite (gallic acid) (ferulic acid). Spectral analysis was used to further purify samples of metabolites after solvent extraction and column chromatography. By comparing their spectrum data to those provided in the literature, spectra (NMR) for isolated metabolites were established.

The interaction of AR-A014418 with the active site of GSK-3β has been studied and displayed in 2D and 3D style **(Figure 1b)**. The proposed binding mode of AR-A014418 revealed an affinity value of -7.62 kcal/mol that demonstrated the important interactions of AR-A014418 at the active site of GSK-3β.

AR-A014418 mediated two H-bonding interactions in order to bind with the key hot spot VAL135 of the receptor via amidic NH and thiazole ring nitrogen with a distance of 2.52Å and 2.88Å, respectively. Besides hydrophobic interactions, the central phenyl moiety interacted with ILE62 residue through arene-H interaction with a distance of 4.12Å.

The proposed binding mode of gallic acid (affinity value of -7.31 kcal/mol) **(Figure 1c)** revealed that gallic acid mediated two H-bonding interactions with VAL135 residue via carboxyl group OH with a distance of 2.92Å and 3.03Å respectively, while the central phenyl moiety binds with ILE62 residue through arene-H interaction with a distance of 4.46Å. The proposed binding mode of protocatechuic acid (affinity value of -6.55 kcal/mol) **(Figure 1d)** revealed that protocatechuic acid possessed H-bonding interaction with VAL135 residue via hydroxyl group with a distance of 2.78 Å. In addition, the central phenyl moiety binds with ILE62 residue through arene-H interaction with a distance of 4.24Å. Finally, the binding mode of ferulic acid (affinity value of -3.21 kcal/mol) **(Figure 1e)** revealed that ferulic acid possessed H-bonding interaction with VAL135 residue via hydroxyl group with a distance of 3.04 Å.

As further documentation of our results, the neuroprotective potential of the tested metabolites was evaluated using the mRTBI model. The tested metabolites confirmed their neuroprotective ability via their anti-inflammatory and anti-dementia and by modulating both GSK3B and DKK-1(signaling molecule). Besides, these results as well involved an improvement in the behavioral outcome and histological structure. When the skull is subjected to enough external force to cause brain damage, a traumatic brain injury (TBI) develops. The severity of TBI can vary, but moderate TBI (mTBI), which makes up around 80% of all cases in the US, is the most prevalent type. While more serious TBI entails a combination of axonal degeneration and neuronal cell loss [22], in mTBI, a negligible loss of consciousness and minimal neuropathology can be observed. However, it is challenging to identify mTBI after a single incidence. The majority of cognitive and behavioral abnormalities often improve within weeks of the head injury in only a small number of instances, necessitating longer recovery times [23-25]. Mostly, frequent exposure to the same situation may cause the brain to develop a more serious, enduring disease of mild repetitive TBI (mRTBI) [26]. More severe and protracted cognitive, motor, and behavioral complications are associated with mRTBI and may last for months and even years [27, 28]. Persistent brain injuries are evident even after symptoms of remission, a finding that carries an increased risk of dementia, Alzheimer's disease (AD), chronic traumatic encephalopathy (CTE), and Parkinson's disease (PD) [29, 30].

Histopathological examination received some engrossment in the current work, as post-concussion dementia was previously misdiagnosed in athletes as AD prior to the prevalence of the term CTE [4], where our records showed a histological alteration of the brain with mild brain injury mTBI **(Figure 4)**; these results were vacuolated granular cells and degenerations of external granular layer C1 and some pycnotic changes of pyramidal cells PPYC of polymorphic layer C4 and C2 and C3. While these results were more severe with the second group of repetitive brain injury RTBI-10 **(Figure 4)**, showed marked vacuolation and pyknotic changes of granular cells of both external layer C1 and inner C2 layer and pyknotic changes of pyramidal cells (PPYC) and some karyolysis changes (KGC) of granular cells and infiltrations of inflammatory cells with dilated and congested blood vessels CBV. These results are in agreement with the results published before [22]. They show that mild blast-related TBI caused morphological alterations in the model mice's parietal cortex and hippocampus and that there was a substantial decrease in dendritic density and distribution. They also showed that the dendritic branching in the parietal cortex and hippocampus had diminished. We also noticed declines in dendritic length and complexity, which may indicate a reduction in connection within the hippocampus, along with the reduced dendritic branching inside the hippocampus found in this study.

Our findings also followed the results of [31], where TBI causes degeneration of the hippocampi and other brain regions, and the degree of atrophy is correlated with the degree of brain injury [32]. The hippocampal region of the brain, which is crucial for cognition, is extremely vulnerable to damage [33]. Compared to its other divisions, the hippocampus has a lower capillary mass [34]. TBI makes hippocampal pyramidal neurons more susceptible to death. Therefore, its damage will be seen a few days after the rat's injury.

In addition to histo-findings, animals exposed to 5 repetitive hits showed behavioral alteration as marked herein using an open field test. Additionally, this effect extended to biochemical markers, where the mRTBI-10 group showed a significant increase in cortical contents of phosphorylated Tau (pTau), inflammatory markers, and signaling molecules such as GSK3B and DKK-1; Post-treatment with gallic acid (GA) after mRTBI showed marked improvement in the histological structure of the hippocampus, see **Figure 5** that showed more or less normal histoarchitecture of hippocampus regions with a mild frequency of pyknotic pyramidal cells (PPYC) with normal appearance of neurons and glial cells showing astrocyte (AST) in contact with blood vessel (BV). Furthermore, GA abated *p*-TAU, TNF-α, IL-6, GSK3β, and DKK-1, showing anti-dementia, anti-inflammatory and antiapoptotic activity. These results are in agreement with previous studies that reported that GA has anti-inflammatory and antioxidant effects and saves brain tissue after cerebral ischemia and AD [35-37]. Additionally, a previous study showed that giving rats GA could help with cognitive deficiencies caused by rat brain injury. The antioxidant in GA is thought to be responsible for the compound's cognitive-improving and neuroprotective effects [36], which are consistent with the study's behavioral recording and Tau (a dementia marker) test results. PCA-treated rats demonstrated a marked improvement in hippocampus histoarchitecture **(Figure 5)**, along with the tau protein, inflammatory, and apoptotic markers modulation. This concomitant with the results that reported that PCA treatment protected neuronal loss after TBI by reducing oxidative damage, microglial activation, and glutathione depletion. These three factors together prevented the neuronal loss [13]. Furthermore, PCA has been recognized as a cytoprotective agent *in-vivo* and *in-vitro* through its anti-apoptotic, anti-oxidative, and anti-inflammatory effects [38].

The result of the present study also showed a mild ameliorative effect of FA in the mRTBI model **(Figure 6)**. This is in agreement with the results reported that Ferulic acid protects brain tissue from MCAO-induced apoptotic cell death and has neuroprotective effects in focal cerebral ischemia [39, 40]. FA also confirmed neuroprotection by modulating the investigated markers and enhancing behavior outcomes compared to animals exposed to repeated trauma. In line with our findings, a previous study documented the neuroprotective and anti-inflammatory effects of FA [41, 42].

## Conclusion

Our results strongly suggest that GA, PCA, and FA have therapeutic potential for preventing TBI-induced brain damage. It would be wise to carry out pre-clinical trials of these experimental investigations to help stop the clinical symptoms of mRTBI-CTE.

**Acknowledgments:** The authors thank Helwan and October 6th Universities for the facilities introduced during this work.

**Conflict of interest:** None

**Financial support:** None

**Ethics statement:** Institutional Animal Care and Use Committee (HU-IACUC) Faculty of Science, Helwan University, Approval Number: HU-IACUC/Z/AA1019-17.

## References

1. Hyder AA, Wunderlich CA, Puvanachandra P, Gururaj G, Kobusingye OC. The impact of traumatic brain injuries: a global perspective. NeuroRehabilitation. 2007;22(5):341-53.
2. Bryant RA, O'donnell ML, Creamer M, McFarlane AC, Clark CR, Silove D. The psychiatric sequelae of traumatic injury. Am J Psychiatry. 2010;167(3):312-20.
3. Smith DH, Johnson VE, Trojanowski JQ, Stewart W. Chronic traumatic encephalopathy—confusion and controversies. Nat Rev Neurol. 2019;15(3):179-83.
4. Van Ommeren R, Hazrati LN. Pathological Assessment of Chronic Traumatic Encephalopathy: Review of Concepts and Methodology. Acad Forensic Pathol. 2018;8(3):555-64. doi:10.1177/1925362118797729
5. Ojo JO, Mouzon BC, Crawford F. Repetitive head trauma, chronic traumatic encephalopathy and tau: Challenges in translating from mice to men. Exp Neurol. 2016;275:389-404.
6. Baugh CM, Stamm JM, Riley DO, Gavett BE, Shenton ME, Lin A, et al. Chronic traumatic encephalopathy: neurodegeneration following repetitive concussive and subconcussive brain trauma. Brain Imaging Behav. 2012;6(2):244-54.
7. Salter R, Beshore DC, Colletti SL, Evans L, Gong Y, Helmy R, et al. Microbial biotransformation–an important tool for the study of drug metabolism. Xenobiotica. 2019;49(8):877-86.
8. Chadni M, Flourat AL, Reungoat V, Mouterde LM, Allais F, Ioannou I. Selective extraction of sinapic acid derivatives from mustard seed meal by acting on pH: toward a high antioxidant activity rich extract. Molecules. 2021;26(1):212.
9. Ibrahim HA, Soliman HS, Hamed FM, Marrez DA, Othman SM. Antibacterial activity of vanillic acid and catechol produced by microbial biotransformation of caffiec acid. J Pharm Sci Res. 2020;12(6):740-3.

10. Albert-Weißenberger C, Várrallyay C, Raslan F, Kleinschnitz C, Sirén AL. An experimental protocol for mimicking pathomechanisms of traumatic brain injury in mice. Exp Transl Stroke Med. 2012;4(1):1-5.
11. El-Gazar AA, Soubh AA, Mohamed EA, Awad AS, El-Abhar HS. Morin post-treatment confers neuroprotection in a novel rat model of mild repetitive traumatic brain injury by targeting dementia markers, APOE, autophagy and Wnt/β-catenin signaling pathway. Brain Res. 2019;1717:104-16.
12. Koh PO. Ferulic acid prevents the cerebral ischemic injury-induced decrease of Akt and Bad phosphorylation. Neurosci Lett. 2012;507(2):156-60.
13. Lee SH, Choi BY, Lee SH, Kho AR, Jeong JH, Hong DK, et al. Administration of protocatechuic acid reduces traumatic brain injury-induced neuronal death. Int J Mol Sci. 2017;18(12):2510.
14. Yang YH, Wang Z, Zheng J, Wang R. Protective effects of gallic acid against spinal cord injury-induced oxidative stress. Mol Med Rep. 2015;12(2):3017-24.
15. Nazeam JA, Ragab GM, El-Gazar AA, El-Mancy SS, Jamil L, Fayez SM. Topical Nano Clove/Thyme Gel against Genetically Identified Clinical Skin Isolates: In Vivo Targeting Behavioral Alteration and IGF-1/pFOXO-1/PPAR γ Cues. Molecules. 2021;26(18):5608. doi:10.3390/molecules26185608
16. Ibrahim RR, Ibrahim HA, Shabana SS, El-Hosari DG, Ali SA, Mahgoub S, et al. New phenolic compounds from Calothamnus quadrifidus R. Br. aerial parts and their antioxidant activity. Nat Prod Res. 2021;35(23):5183-91.
17. Daniel IJ, Innocent E, Sempombe J, Mugoyela V, Fossen T. Isolation and Characterization of Larvicidal Phenolic Acids from Kotschya thymodora Leaves. J Appl Sci Environ Manag. 2020;24(8):1483-8.
18. Phukan S, Babu VS, Kannoji A, Hariharan R, Balaji VN. GSK3β: role in therapeutic landscape and development of modulators. Br J Pharmacol. 2010;160(1):1-9.
19. Chang YT, Chen CL, Lin CF, Lu SL, Cheng MH, Kuo CF, et al. Regulatory role of GSK-3 β on NF- κ B, nitric oxide, and TNF- α in group A streptococcal infection. Mediators Inflamm. 2013;2013:720689.
20. Su TR, Lin JJ, Tsai CC, Huang TK, Yang ZY, Wu MO, et al. Inhibition of melanogenesis by gallic acid: Possible involvement of the PI3K/Akt, MEK/ERK and Wnt/β-catenin signaling pathways in B16F10 cells. Int J Mol Sci. 2013;14(10):20443-58.
21. Usha T, Goyal AK, Narzary D, Prakash L, Wadhwa G, Babu D, et al. Identification of bioactive glucose-lowering compounds of methanolic extract of Hodgsonia heteroclita fruit pulp. Front Biosci - Landmark. 2018;23(5):875-88.
22. Ratliff WA, Mervis RF, Citron BA, Schwartz B, Rubovitch V, Schreiber S, et al. Effect of mild blast-induced TBI on dendritic architecture of the cortex and hippocampus in the mouse. Sci Rep. 2020;10(1):1-8.
23. Lovell MR, Collins MW, Iverson GL, Field M, Maroon JC, Cantu R, et al. Recovery from mild concussion in high school athletes. J Neurosurg. 2003;98(2):296-301.
24. McCrea M, Guskiewicz KM, Marshall SW, Barr W, Randolph C, Cantu RC, et al. Acute effects and recovery time following concussion in collegiate football players: the NCAA Concussion Study. Jama. 2003;290(19):2556-63.
25. Losoi H, Silverberg ND, Wäljas M, Turunen S, Rosti-Otajärvi E, Helminen M, et al. Recovery from mild traumatic brain injury in previously healthy adults. J Neurotrauma. 2016;33(8):766-76.
26. Guskiewicz KM, McCrea M, Marshall SW, Cantu RC, Randolph C, Barr W, et al. Cumulative effects associated with recurrent concussion in collegiate football players: the NCAA Concussion Study. Jama. 2003;290(19):2549-55.
27. De Beaumont L, Theoret H, Mongeon D, Messier J, Leclerc S, Tremblay S, et al. Brain function decline in healthy retired athletes who sustained their last sports concussion in early adulthood. Brain. 2009;132(3):695-708.
28. De Beaumont L, Henry LC, Gosselin N. Long-term functional alterations in sports concussion. Neurosurg Focus. 2012;33(6):E8.
29. Nakamura T, Hillary FG, Biswal BB. Resting network plasticity following brain injury. PloS one. 2009;4(12):e8220.
30. Mayer AR, Mannell MV, Ling J, Gasparovic C, Yeo RA. Functional connectivity in mild traumatic brain injury. Hum Brain Mapp. 2011;32(11):1825-35.
31. Mirshekar MA, Sarkaki A, Farbood Y, Naseri MK, Badavi M, Mansouri MT, et al. Neuroprotective effects of gallic acid in a rat model of traumatic brain injury: behavioral, electrophysiological, and molecular studies. Iran J Basic Med Sci. 2018;21(10):1056.
32. Harris TC, de Rooij R, Kuhl E. The shrinking brain: cerebral atrophy following traumatic brain injury. Ann Biomed Eng. 2019;47(9):1941-59. doi:10.1007/s10439-018-02148-2
33. Farkas E, Luiten PG, Bari F. Permanent, bilateral common carotid artery occlusion in the rat: a model for chronic cerebral hypoperfusion-related neurodegenerative diseases. Brain Res Rev. 2007;54(1):162-80.
34. Perosa V, Priester A, Ziegler G, Cardenas-Blanco A, Dobisch L, Spallazzi M, et al. Hippocampal vascular reserve associated with cognitive performance and hippocampal volume. Brain. 2020;143(2):622-34. doi:10.1093/brain/awz383
35. Sun J, Li YZ, Ding YH, Wang J, Geng J, Yang H, et al. Neuroprotective effects of gallic acid against hypoxia/reoxygenation-induced mitochondrial dysfunctions in vitro and cerebral ischemia/reperfusion injury in vivo. Brain Res. 2014;1589:126-39.
36. Korani MS, Farbood Y, Sarkaki A, Moghaddam HF, Mansouri MT. Protective effects of gallic acid against chronic cerebral hypoperfusion-induced cognitive deficit and brain oxidative damage in rats. Eur J Pharmacol. 2014;733:62-7.

37. Hajipour S, Sarkaki A, Farbood Y, Eidi A, Mortazavi P, Valizadeh Z. Effect of gallic acid on dementia type of Alzheimer disease in rats: electrophysiological and histological studies. Basic Clin Neurosci. 2016;7(2):97.
38. Zhang S, Gai Z, Gui T, Chen J, Chen Q, Li Y. Antioxidant Effects of Protocatechuic Acid and Protocatechuic Aldehyde: Old Wine in a New Bottle. Evid Based Complement Alternat Med. 2021;2021:6139308. doi:10.1155/2021/6139308
39. Yin X, Zhang X, Lv C, Li C, Yu Y, Wang X, et al. Protocatechuic acid ameliorates neurocognitive functions impairment induced by chronic intermittent hypoxia. Sci Rep. 2015;5(1):1-4.
40. Krzysztoforska K, Mirowska-Guzel D, Widy-Tyszkiewicz E. Pharmacological effects of protocatechuic acid and its therapeutic potential in neurodegenerative diseases: Review on the basis of in vitro and in vivo studies in rodents and humans. Nutr Neurosci. 2019;22(2):72-82.
41. Ren Z, Zhang R, Li Y, Li Y, Yang Z, Yang H. Ferulic acid exerts neuroprotective effects against cerebral ischemia/reperfusion-induced injury via antioxidant and anti-apoptotic mechanisms in vitro and in vivo. Int J Mol Med. 2017;40(5):1444-56.
42. Hadibarata T, Syafiuddin A, Al-Dhabaan FA, Elshikh MS. Biodegradation of Mordant orange-1 using newly isolated strain Trichoderma harzianum RY44 and its metabolite appraisal. Bioprocess Biosyst Eng. 2018;41(5):621-32.